IX International Conference on Particle-Based Methods
PARTICLES 2025
J. Bonet, M. Cremonesi, A. Franci, A. Gil (Eds)

A COMPARATIVE STUDY OF A CONVENTIONAL AND MODERN TRANSPORT-VELOCITY SPH SCHEME IN A REACTIVE MASS TRANSFER PROBLEM

KARTHIK. V. MUTHUKUMAR[*], CIHAN ATES[†], NIKLAS BÜRKLE[*], MARKUS WICKER[*], RAINER KOCH[*], HANS-JÖRG BAUER[*]

[*] Institute of Thermal Turbomachinery
Karlsruhe Institute of Technology
Kaiserstraße 12, 76137 Karlsruhe, Germany
e-mail: karthik.muthukumar@kit.edu, www.its.kit.edu

[†] Hoffmann Group
Haberlandstraße 55, 81241 Munich
email: cihan.ates@hoffmann-group.com, www.hoffmann-group.com

Keywords: Smoothed Particle Hydrodynamics, Advection-Diffusion equation, Laminar Flow Reactor, SPH with transport velocity.

Abstract. The advection-diffusion equation is fundamental to modeling mass transfer in various engineering applications, including solute transport in catalytic reactors, pollutant dispersion in environmental flows, and drug delivery in biological tissues. These problems often span a wide range of transport regimes, making accurate and robust numerical solutions essential for predictive modeling and design. In this work, we investigate two Weakly Compressible Smoothed Particle Hydrodynamics (WCSPH) approaches, a conventional SPH and a modern SPH with transport velocity, for modeling mass transport in a Laminar Flow Reactor (LFR), which includes advection, diffusion, and reaction effects. The study examines three Peclet numbers (Pe = 10, 1000, and 100,000), corresponding to diffusion-influenced, mixed, and advection-dominated transport regimes, respectively. Numerical results are benchmarked against COMSOL Multiphysics®. The modern SPH method demonstrates improved performance over the conventional SPH in low to moderate Peclet regimes, exhibiting reduced particle disorder, enhanced stability, and more accurate diffusion resolution. At high Peclet numbers, both approaches yield comparable results, though the modern SPH shows improved convergence and outlet concentration predictions. These findings highlight the potential of the implemented modern SPH approach for improved modeling of mass transfer in chemical reactors, particularly in diffusion-sensitive applications.

1 INTRODUCTION

The advection-diffusion equation, often extended with source or sink terms as the species conservation equation (Equation 1), governs the transport of scalar quantities such as chemical concentrations in fluid systems. It encompasses advection ($\nabla.(\vec{u}C)$), diffusion ($D\nabla^2C$), accumulation $\left(\frac{dC}{dt}\right)$, and reaction ($kC$) terms, each contributing to the complexity of numerical

modeling across varying transport regimes. In low Peclet number (Pe) flows, characteristic of microfluidic devices, electrochemical systems such as fuel cells, packed beds, porous media, and biological tissues, diffusion effects dominate. Resolving these diffusion-dominated regimes poses challenges in particle-based solver frameworks, due to the sensitivity of the second-order diffusion operator ($\nabla^2 C$) to particle disorder [1]. At high Pe numbers, typical of systems such as high-speed reactors, certain combustion processes, and large-scale circulatory flows, advection dominates over diffusion. In such regimes, accurate resolution of the velocity field is essential for predicting species transport, while in low Pe number systems, dominated by diffusion, the stability and consistency of spatial derivatives become more critical. These contrasting requirements place significant demands on numerical methods used to solve the advection-diffusion-reaction equation, particularly in maintaining solution accuracy across a broad range of transport regimes.

$$\frac{dC}{dt} = D\nabla^2 C - \nabla.(\vec{u}C) - kC \tag{1}$$

The conventional Weakly Compressible SPH (WCSPH) formulation employs a background pressure to maintain particle order and advects particles using local fluid velocities, but suffers from several well-known limitations [2], particularly non-uniform particle distributions, spurious pressure oscillations, and degradation of numerical accuracy in both advection and diffusion-dominated regimes. To address these issues, some modern SPH formulations employ a transport velocity, distinct from the fluid velocity, enabling improved control over particle trajectories and spatial regularity. In this work, we apply the WCSPH scheme, based on Werdelmann et al. [3]. Here, the particle shifting algorithms introduced by Lind et al. [4] redistribute particles according to a Fickian diffusion model. This approach leads to enhanced particle uniformity, improved resolution of the diffusion term, and more stable velocity fields, especially in regimes where particle disorder critically affects accuracy.

Applications of SPH to diffusion and mass transfer problems have been studied by various authors. Cleary and Monaghan [5] first explored its use in heat conduction. Zhu and Fox [6,7] applied SPH to model mass transport in periodic porous structures, while Tartakovsky et al. [8,9] investigated miscible displacement and reactive transport in fractured media. For advection-dominated flows, Aristodemo et al. [11], building on Monaghan's formulation [10], proposed an SPH discretization of the advection–diffusion equation using harmonic means to handle discontinuous diffusion coefficients.

Building upon these developments, the present work combines the diffusion formulation by Tartakovsky et al. [8,9] with the advection treatment introduced by Aristodemo et al. [11], and incorporates a first-order homogeneous reaction term to form a complete species transport model. This modelling approach is implemented in both conventional and modern SPH frameworks and applied to a Laminar Flow Reactor (LFR), which serves as a representative benchmark for coupled advection-diffusion-reaction processes. By conducting simulations across a range of Peclet numbers, spanning diffusion-dominated, mixed, and advection-dominated regimes, we assess the accuracy and suitability of both SPH approaches. The study aims to identify the transport regimes in which the modern SPH with transport velocity offers significant improvements, particularly in the context of engineering systems where precise mass transfer prediction is critical.

2 NUMERICAL METHODS

This study compares a conventional Weakly Compressible Smoothed Particle Hydrodynamics (WCSPH) formulation with a modern WCSPH variant, similar to the scheme proposed by Werdelmann et al. [3]. An isothermal, viscous fluid flow with constant dynamic viscosity is assumed throughout. In the WCSPH framework, pressure is computed from density using Tait's equation of state, which relates pressure p to the local density ρ and ρ_0, reference speed of sound c_0, and barotropic exponent γ:

$$p = \frac{\rho_0 c_0^2}{\gamma}\left[\left(\frac{\rho}{\rho_0}\right)^{\gamma} - 1\right]. \tag{2}$$

Density is evaluated using a summation interpolant, as described by Hu and Adams [12], based on neighboring particle contributions via a smoothing kernel,

$$\rho_i = m_i \sum_j \nabla_i W_{ij}. \tag{3}$$

In SPH, the computational domain is discretized into particles, each carrying a fixed mass. Volume V is determined from the particle mass m and its current density ρ, ensuring mass conservation by construction,

$$V = \frac{m}{\rho}. \tag{4}$$

The temporal derivative of the velocity (Equation 5) is the sum of the pressure gradient $\vec{a}_i^{\,p}$ (Equation 6) from Colagrossi et al. [13] and the viscous term $\vec{a}_i^{\,\mu}$ (Equation 7) from Szewc et al. [14]. This setup is referred to as the conventional SPH in this study.

$$\frac{d\vec{u}_i}{dt} = \vec{a}_i^{\,p} + \vec{a}_i^{\,\mu}, \tag{5}$$

$$\vec{a}_i^{\,p} = \langle\frac{\overrightarrow{\nabla p}}{\rho}\rangle_i = \frac{1}{\rho_i}\sum_j \frac{m_j}{\rho_j}\left(p_i + p_j\right)\nabla_i W_{ij}, \tag{6}$$

$$\vec{a}_i^{\,\mu} = \langle\frac{\overrightarrow{\nabla \tau}}{\rho}\rangle_i = m_j \sum_j 8\frac{\left(\nu_j + \nu_j\right)}{\rho_i + \rho_j}\frac{\vec{r}_{ij}.\,\nabla_i W_{ij}}{\left|\vec{r}_{ij}\right|^2 + \eta^2}\vec{u}_{ij}. \tag{7}$$

In contrast, in the modern SPH setup, the particles are advected with a transport velocity $\vec{\hat{u}} = \vec{u} + \delta\vec{u}$, where $\delta\vec{u}$ is the shift velocity. Here, we calculate the temporal density and velocity as,

$$\frac{d\rho_i}{dt} = -\rho_i \sum_j V_j\left(\vec{u}_j - \vec{u}_i\right)\nabla_i W_{ij} + \delta h D_i^{\rho}, \tag{8}$$

$$\frac{d\vec{u}_i}{dt} = \vec{a}_i^{\,p} + \vec{a}_i^{\,\mu}. \tag{9}$$

The density diffusion term $\delta h D_i^{\rho}$ is as proposed by Ferrari et al. [16], scaled with the geometrical smoothing length h and with $\delta = 0.1$. The shifting velocity $\delta\vec{u}$ is computed from the particle concentration gradient as in Lind et al.[4], using the smoothing length, h.

$$\delta\vec{u} = -\epsilon\frac{h^2}{\delta t}\sum_j V_j\,\nabla_i W_{ij}. \tag{10}$$

While both SPH approaches differ in how position, and density are updated, both approaches use the same formulation for species concentration transport. The time integration is performed using an explicit mid-point scheme. The advection-diffusion-reaction equation is discretized

using the method of Tartakovsky et al. [9] for the diffusion term, and the scheme of Aristodemo et al. [10] for the advection term. To improve numerical stability and accuracy, particularly under variable-density conditions, the advection-diffusion-reaction equation (Equation 1) is reformulated [10], introducing density-weighted divergence operators for both the diffusive and convective fluxes as,

$$\frac{dC}{dt} = \frac{1}{\rho}\nabla.(D\rho\nabla C) - \frac{1}{\rho}[\nabla.(\rho\vec{u}C) - \vec{u}C.\nabla\rho] - kC. \tag{11}$$

This equation is discretized in the SPH form as,

$$\frac{dC_i}{dt} = \sum_j \frac{\left(m_j\rho_i D_i + m_i\rho_j D_j\right)}{\rho_i\rho_j} \frac{\vec{r}_{ij}.\nabla_i W_{ij}}{\left|\vec{r}_{ij}\right|^2+\eta^2} C_{ij} + \sum_j m_j \frac{C_i}{\rho_i}\vec{u}_{ij}.\vec{r}_{ij}.\nabla_i W_{ij} - kC_i. \tag{12}$$

3 PROBLEM DEFINITION

For this study, we use a 2D Laminar Flow Reactor with a homogenous first-order reaction of reaction rate k = 1.462 $1/s$. The reactor geometry is a cylindrical pipe of length 100mm and diameter 10mm (see Figure 1). The whole domain is initialized with a uniform species of concentration $C(x, r, t=0) = 2\,mol/m^3$. Also, the concentration at the inlet boundary is set to $C = 2\,mol/m^3$, and a no-flux boundary condition $\frac{\partial C}{\partial r} = 0$ at the walls. The velocity field is fully developed and prescribed analytically using the parabolic Hagen–Poiseuille profile:

$$u(r) = u_{max}\left(1 - \left(\frac{r}{R}\right)^2\right), \text{with } u_{max} = 2u_{bulk}, \tag{13}$$

where R is the pipe radius and u_{bulk} is the average axial velocity. The flow medium is air at room temperature, and flow parameters are chosen to ensure laminar conditions throughout the domain. To investigate the performance of both SPH schemes across different transport regimes, simulations are carried out at three Peclet numbers: Pe = 10, 1000, and 100,000, where the Peclet number *Pe* is defined as,

$$Pe = \frac{advection\ rate}{diffusion\ rate} = \frac{uL}{D}. \tag{14}$$

Where *u* is the characteristic velocity, *L* is the characteristic length, and *D* is the diffusion coefficient of the species. These three configurations correspond to diffusion-dominated, mixed, and advection-dominated regimes, respectively. A constant bulk velocity of 100 mm/s is maintained across all cases, and the diffusion coefficient is varied accordingly to achieve the desired Peclet number. The parameter configurations are summarized in Table 1. In this study, we set the parameter $\epsilon = 0.5$ (in Equation 10) and the background pressure to 0.025.

Table 1: Peclet number configurations

Peclet number	Bulk velocity	Diffusion coefficient
10	100 mm/s	10^3 mm^2/s
1000	100 mm/s	10 mm^2/s
100000	100 mm/s	0.1 mm^2/s

A high-fidelity numerical solution is obtained using COMSOL Multiphysics® (v6.1.0),

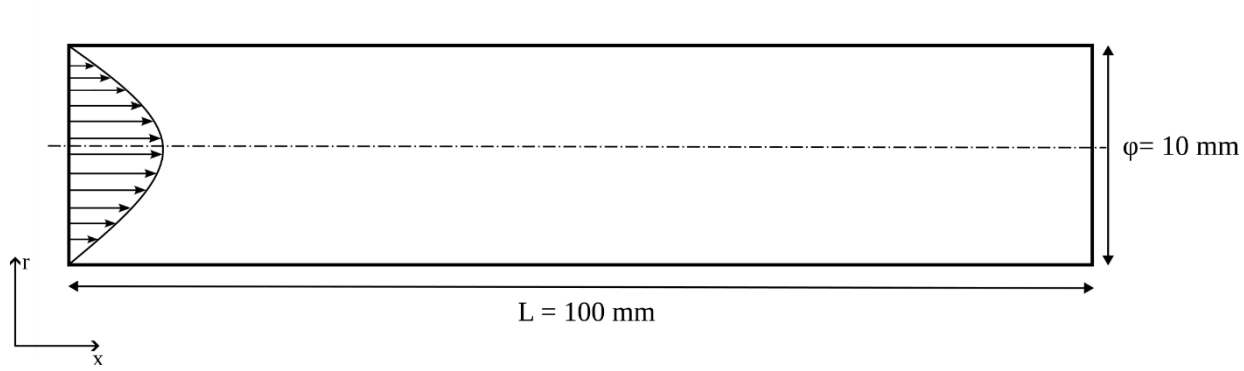

Figure 1: LFR Geometry

which serves as the reference for error quantification. The reference model is solved in steady state using the "Laminar Flow" (spf) and "Transport of Diluted Species" (tds) modules. A structured, mapped mesh is employed, consisting of 1600 elements along the axial direction and 160 elements along the radial direction (corresponding to a cell size of dx=62.5μm). The converged COMSOL solution is used to evaluate the accuracy of the SPH-based methods. The concentration profiles are extracted along three probe lines: at the centerline (r = 0), and at two symmetric radial locations (r=±2.5mm). These profiles are compared at multiple cross-sections along the axial length of the reactor. All SPH simulations are run using a Quintiv b-spline with a smoothing length $h=dx$ until t=10s, at which a steady-state is reached with the discretization schemes described in the previous section and corresponding spatial resolutions provided in Table 2.

Table 2: Particle resolutions used in SPH solutions

Spatial resolution	Particle size
Coarse	dx=500μm
Mid	dx=250μm
Fine	dx=125μm

3 RESULTS AND DISCUSSION

Figure 2 shows the contour line plot of the concentration fields at a steady state for the three Peclet numbers, computed using COMSOL and both SPH approaches (at t = 10s), and presents a qualitative comparison. The black, red, and blue lines correspond to the contour lines from COMSOL, modern SPH, and conventional SPH, respectively. The contour lines os the SPH are from the highest resolution (dx = 125μm). As expected, the parabolic velocity profile significantly influences the shape of the scalar field. At low Peclet numbers (Pe = 10), the concentration becomes more uniform across the cross-section due to strong diffusion. In contrast, at high Peclet numbers (Pe=100,000), advection dominates, leading to sharper concentration gradients near the centreline and pronounced axial transport. For Pe=10 and 1000, the modern SPH predicts the concentration fields better compared to conventional SPH, consistent with enhanced diffusion and better resolution of second-order derivatives. At Pe=100,000, on the other hand, advection dominates the transport process. Due to the parabolic

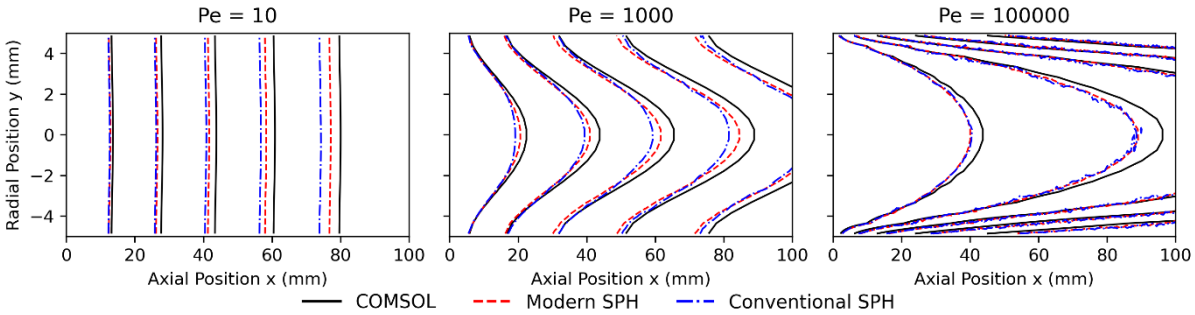

Figure 2: Comparison of the evolution of the concentration profiles for the COMSOL, modern and conventional SPH. The top, middle and bottom row corresponds to Pe = 10, 1000, 100000

profile, fluid elements near the centreline are transported downstream rapidly, while particles near the wall, experiencing lower velocities, exhibit enhanced diffusion owing to longer residence times. This results in asymmetric diffusion effects, which are more accurately captured by the modern SPH (see relative error plots).

Figures 3, 4, and 5 show the relative error in species concentration along the reactor length

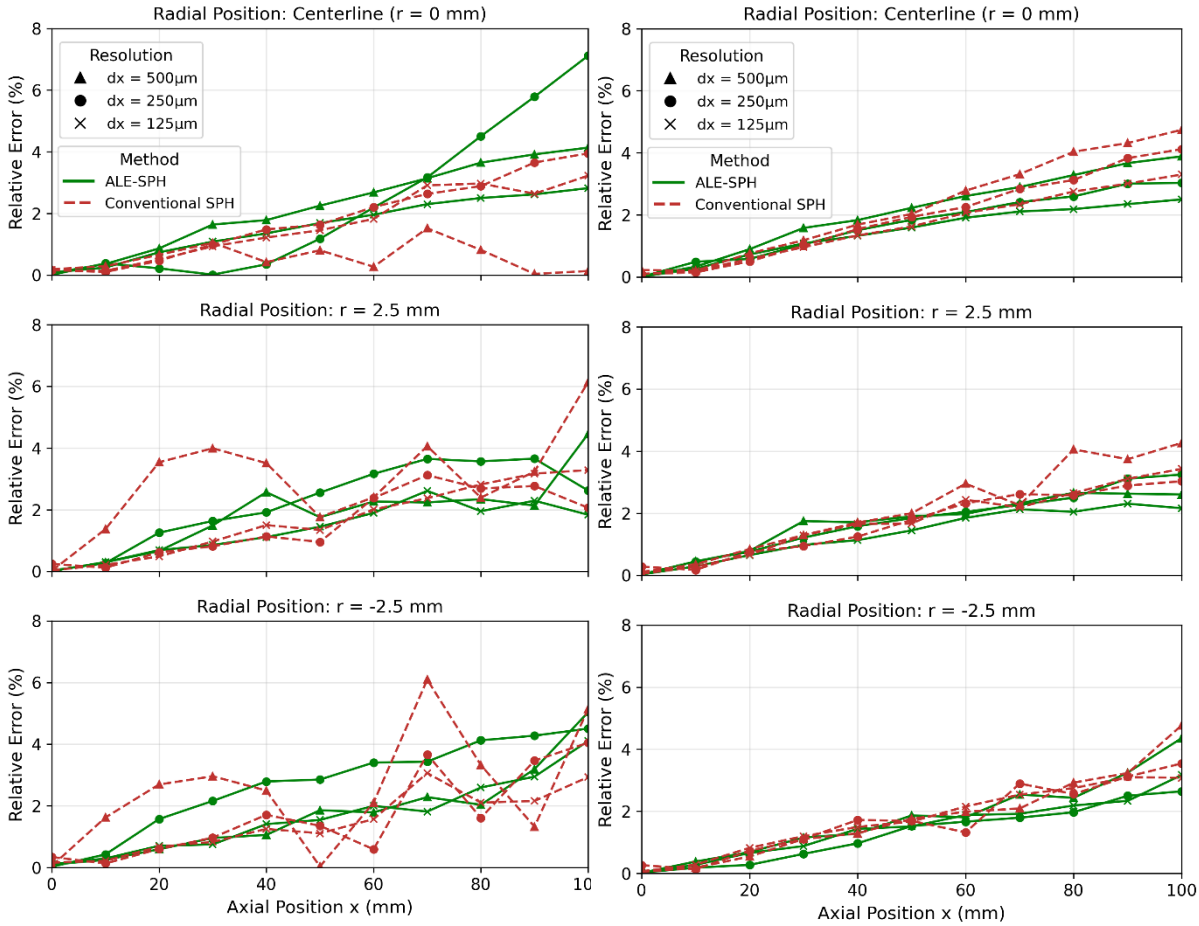

Figure 3: Relative error for both SPH approaches at Pe=100000

Figure 4: Relative error for both SPH approaches at Pe=1000

at three radial positions: the centerline (r=0 mm) and two off-center locations (r=±2.5 mm). These probe lines help evaluate the symmetry and accuracy of each SPH approach with respect to the COMSOL reference solution. At high Peclet number (Pe=100,000; Figure 3), both SPH schemes yield comparable error magnitudes, but the modern SPH demonstrates improved spatial symmetry and convergence, particularly near the outlet. The conventional SPH scheme shows fluctuating errors, primarily due to inaccuracies in the velocity field caused by particle disorder. At intermediate Peclet number (Pe=1000; Figure 4), the modern SPH scheme continues to outperform conventional SPH, although the performance gap is narrower. In this regime, convective transport is still dominant, and the impact of particle disorder is less pronounced than in diffusion-dominated flows. Nevertheless, the modern SPH produces smoother and more symmetric error profiles, indicating better stability. At a low Peclet number (Pe=10; Figure 5), the advantage of the modern SPH becomes most pronounced. The relative error is significantly lower and more consistent across all probe lines. This is attributed to the high sensitivity of the diffusion term (involving a second-order spatial derivative) to particle disorder, which the modern SPH mitigates through its shifting algorithm. Despite using background pressure stabilization, the conventional SPH approach struggles to maintain a uniform particle distribution, leading to larger local errors. These observations are also

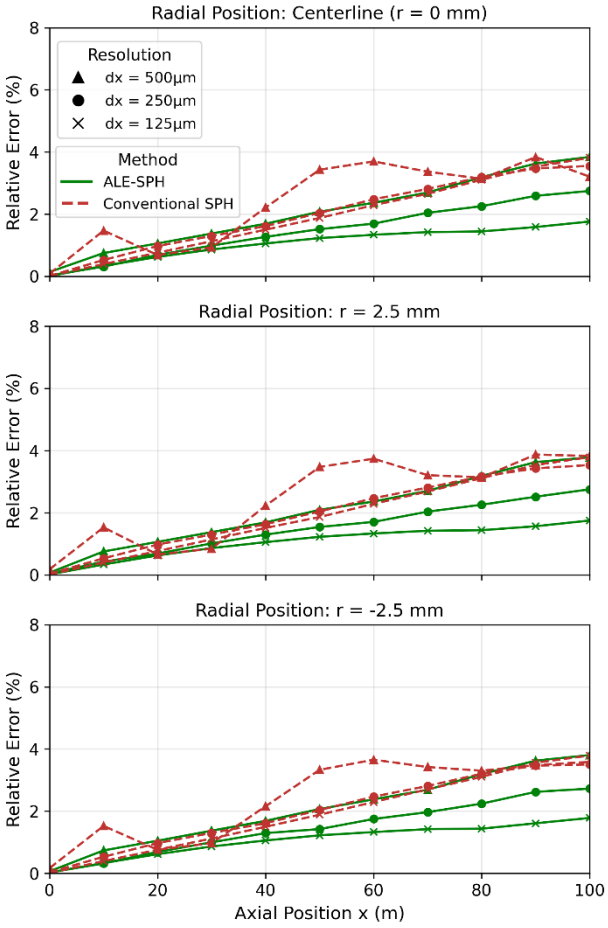

Figure 5: Relative error for both SPH approaches at Pe=10

consistent with the cross-sectional concentration fields shown in Figure 2, where diffusion-dominated flows exhibit smoother profiles and better symmetry under the modern SPH.

Table 3 reports the relative errors of the spatially averaged concentration at x=25mm, 50mm, and 100mm (outlet) for the highest-resolution SPH simulations, with COMSOL serving as the reference. Although the full spatial distribution of species concentration is critical for understanding reactor behavior, particularly in systems involving reaction kinetics or spatially varying source terms, the outlet concentration remains a commonly used performance metric, especially in reactor design and optimization tasks. Across all Peclet numbers, the modern SPH approach yields lower relative errors in the outlet concentration at the other two positions (x=25mm and 50mm) compared to the conventional SPH formulation. The largest difference is observed at Pe=10, where diffusion effects dominate and solution accuracy is more sensitive to particle disorder. At Pe=100,000, where advection dominates, the error at the outlet is also lower for the modern SPH, though both methods yield similar trends. At intermediate Peclet number (Pe=1000), the differences are smaller. These results suggest that the modern SPH may offer improved accuracy in regimes where either diffusion or advection effects are strongly dominant, likely due to its enhanced control over particle distribution.

Table 3: Relative errors of spatially averaged concentrations along the reactor length

Peclet number	Modern SPH			Conventional SPH		
	x=25mm	x=50mm	x=100mm	x=25mm	x=50mm	x=100mm
10	0.74%	1.22%	1.76%	0.94%	1.87%	3.79%
1000	1.08%	1.42%	2.26%	0.88%	1.42%	3.34%
100000	1.55%	0.25%	0.82%	0.26%	0.44%	3.02%

4 CONCLUSIONS

This study evaluated the performance of a conventional and modern SPH formulation for modeling mass transport in a laminar flow reactor across three Peclet numbers (Pe=10, 1000, 100,000). The concentration fields obtained from both methods were compared against a COMSOL reference solution at multiple radial positions and at the reactor outlet. In diffusion-dominated conditions (Pe=10), the implemented modern SPH approach demonstrated improved accuracy over conventional SPH. The enhanced performance is attributed to its particle-shifting mechanism, which mitigates the impact of particle disorder, a key source of error in resolving second-order diffusion terms. At higher Peclet numbers (Pe=1000 and Pe=100,000), where advection dominates, both methods yielded similar trends. However, the modern SPH still exhibited improved convergence behavior and more symmetric error profiles, particularly near the outlet. The outlet concentration predictions, often critical in the design and evaluation of chemical reactors, were more accurate with the modern SPH approach across all Pe numbers. While conventional SPH provides reasonable accuracy in convection-dominated regimes, the implemented modern SPH offers more consistent performance across the full range of transport conditions.

Future work will focus on extending the present comparison to reactive transport systems with nonlinear or spatially varying reaction kinetics, which are common in real-world chemical and biological applications. Additionally, transient analyses could be conducted to evaluate the performance of the modern SPH in time-dependent scenarios. The method's behavior in three-dimensional geometries and complex boundary conditions also warrants further investigation. Finally, incorporating adaptive particle resolution or coupling with multi-scale frameworks could enhance both computational efficiency and accuracy in large-scale simulations.

REFERENCES

[1] Monaghan, J. J. Smoothed particle hydrodynamics. *Annu. Rev. Astron. Astrophys.* (1992) **30**:543-574.

[2] Vacondio, R., Altomare, C., De Leffe, M., Hu, X., Le Touzé, D., Lind, S., Marongiu, J.-C., Marrone, S., Rogers, B. D. and Souto-Iglesias, A. Grand challenges for smoothed particle hydrodynamics numerical schemes. *Comput. Part. Mech* (2021) **8(3)**:575-588.

[3] Werdelmann, B., Koch, R., Krebs, W. and Bauer, H. J. An approach for permeable boundary conditions in SPH. *J. Comput. Phys* (2021) **444**:110562.

[4] Lind, S. J., Xu, R., Stansby, P. K. and Rogers, B. D. Incompressible smoothed particle hydrodynamics for free-surface flows: A generalised diffusion-based algorithm for stability and validations for impulsive flows and propagating waves. *J. Comput. Phys* (2012) **231(4)**:1499-1523.

[5] Cleary, P.W. and Monaghan, J.J. Conduction modelling using smoothed particle hydrodynamics. *J. Comput. Phys* (1999) **148**:227–264.

[6] Zhu, Y. and Fox, P.J. Smoothed particle hydrodynamics model for diffusion through porous media. *Trasp. Porous Media* (2001) **43**:441–471.

[7] Zhu, Y. and Fox, P.J. Simulation of pore-scale dispersion in periodic using smoothed particle hydrodynamics. *J. Comput. Phys* (2002) **182**:622–645.

[8] Tartakovsky, A.M. and Meakin, P. A. smoothed particle hydrodynamics model for miscible flow in three dimensional fractures and the two-dimensional Rayleigh-Taylor instability. *J. Comput. Phys* (2005) **207**:610–624.

[9] Tartakovsky, A.M., Meakin, P., Scheibe, T.D., and West, R.M.E. Simulations of reactive transport and precipitation with smoothed particle hydrodynamics. *J. Comput. Phys* (2007) **222**:654–672.

[10] Monaghan, J.J. Smoothed particle hydrodynamics. *Rep. Prog. Phys* (2005) **68**:1703–1759

[11] Aristodemo, F., Federico, I., Veltri, P. and Panizzo, A. Two-phase SPH modelling of advective diffusion processes. *Environ. Fluid Mech* (2010) **10(4)**:451-70.

[12] Hu, X. Y. and Adams, N. A. A multi-phase SPH method for macroscopic and mesoscopic flows. *J. Comput. Phys* (2006) **213(2)**:844-861.

[13] Colagrossi, A. and Landrini, M. Numerical simulation of interfacial flows by smoothed particle hydrodynamics. *J. Comput. Phys* (2003) **191(2)**:448–475.

[14] Szewc, K., Pozorski, J. and Minier, J.-P. Analysis of the incompressibility constraint in the smoothed particle hydrodynamics method. *Int. J. Numer. Methods Eng* (2012) **92(4)**:343–369.

[15] Ferrari, A., Dumbser, M., Toro, E. F. and Armanini, A. A new 3D parallel SPH scheme for free surface flows. *Comput. Fluids*, (2009) **38(6)**:1203-1217.